

F. Chedeveigne, G. Casalis, O. Léon,
M. Forte, F. Laurendeau, N. Szulga,
O. Vermeersch, E. Piot
(ONERA)

E-mail: Francois.Chevevergne@onera.fr

DOI : 10.12762/2015.AL10-06

Applications of Dielectric Barrier Discharges and Plasma Synthetic Jet Actuators at ONERA

This paper focuses on two plasma actuators, developed at ONERA: the DBD actuator (Dielectric Barrier Discharge) and the PSJ actuator (Plasma Synthetic Jet). At the DMAE (Modeling for Aerodynamics and Energetics Department), DBD actuation is investigated for laminar/transition purposes. The results presented deal with 2D configurations including both experimental and modeling works. As regards the activities on the PSJ actuator, most of the work is dedicated to the detailed characterization of the general physics involved in such an actuator. Similarly to the DBD activities, both experimental and modeling investigations are performed in order to be able to develop efficient control strategies using the PSJ actuator.

Introduction

Over the last two decades, increasing efforts have been made with regard to plasma-based flow and flight control research activities. While some applications decreased in popularity, a considerable potential appeared in small-scale plasma actuators. Contrary to more conventional devices, plasma actuators have no moving parts and offer the possibility of a very fast response in time. The two primary mechanisms of plasma-based flow control include the generation of body forces and thermal effects. In the first category, a non-thermal plasma actuator, called a DBD (Dielectric Barrier Discharge) actuator, has been extensively studied. It is based on the generation of a non-equilibrium surface discharge that results in a body-force parallel to the wall in which the device is inserted. In the second category, the Applied Physics Laboratory of Johns Hopkins University initially developed the SparkJet actuator, which generates a discharge in a small cavity covered by a millimeter nozzle protruding from the wall. A thermal plasma is produced in order to locally increase the pressure and temperature of the surrounding gas in the cavity, inducing the formation of a synthetic jet through the nozzle.

ONERA has developed plasma actuators of both types over the last decade, namely DBD and PSJ (Plasma Synthetic Jet) actuators. Several applications have been explored for these actuators, ranging from transition delay to flow separation control, through jet noise reduction. All of them concern subsonic flows. For transition or separation applications, flows exhibit small to moderate Reynolds numbers, up

to 1.3 M, corresponding to low Mach numbers. However, for jet noise reduction applications, Mach numbers up to 0.9 have been investigated using the PSJ actuator. Although tangible results have already been obtained with regard to this variety of applications, the fine characterization and the understanding of the mechanisms that drive the effect of those actuators on flows is an essential ingredient to prepare advanced strategies involving active flow control.

This article is a synthesis of the work done at ONERA on these two actuators, focusing on their experimental characterization and on the models developed to simulate their effects on flows.

DBD actuator

An example of a relatively simple plasma actuator is provided by the so-called Dielectric Barrier Discharge (DBD) actuator. Up to now, the DBD actuator considered in the Department has been constituted of two copper electrodes adhered to each face of a dielectric material. An alternating high voltage is applied to one electrode, whereas the other one is grounded. The resulting electric field in the vicinity of the electrodes enables the ionization of the ambient air. Then, the charged particles drift under the effect of the electric field, inducing a local body force (also called “ionic wind”), parallel to the surface of the dielectric. Over the last two decades, many studies have been conducted in order to establish the electrical and mechanical characteristics of this actuator. Most of them are summarized in a recent review from Bénard and Moreau [1].

This ionic wind can be used to control the flow around various aerodynamic configurations. For example, within the European project PLASMAERO [1], the DBD actuator technology has been tested for delaying the boundary layer separation occurring on a NACA15 airfoil mounted with high positive incidence (12.5°) without sweep. Three successive single DBD actuators were mounted next to the wall on the suction side of the model and have been operated separately or simultaneously in order to assess the benefit of a multi-DBD actuation. The results have shown that operating the three actuators simultaneously was more efficient than using a single DBD actuation. During this series of experiments, performed at the Pprime Institute, it has been possible to delay the separation position up to 30% of the chord with multi-DBD actuation. The same experiment has been conducted with PSJ actuators and showed a maximum delay of 45% of the chord.

Another possible use of the DBD actuator currently under investigation in the DMAE, is the control of the laminar-turbulent transition location. In fact, delaying transition over the wings of civil aircraft could be a possible way of reducing fuel consumption by reducing the skin friction drag. This application has been successfully demonstrated on a flat plate, see [3-5], and on an airfoil, see [6-7], for two dimensional configurations and velocities with magnitudes up to 40 m/s.

In addition to these experimental investigations, various numerical approaches have also been conducted, in order to derive a mathematical model for the body force induced by a DBD plasma actuator and to implement it in various fluid solvers (boundary layer codes or RANS codes, for example). These body-force models can be classified into two main categories: phenomenological models, which rely on plasma physics [8-10] and empirical models, which are generally based on velocity measurements in the vicinity of the plasma actuator in quiescent air [11]. However, these empirical models depend strongly on the actuator considered, and particularly on various geometric or electric parameters, leading in practice to new models for each specific DBD actuator.

The remaining part of this section is devoted to the description of recent activities performed at the DMAE on the laminar-turbulent transition delay using a DBD actuator.

Steady and unsteady effect of a DBD actuator

A sketch of a typical DBD actuator used at the DMAE is given in Figure 1, together with its installation on a flat plate.

In this example, both electrodes have the same width and are made from the usual copper tape. The air-exposed electrode is located upstream from the one that is grounded, in order to induce a body force in the main-stream direction. In this case, a dielectric insert made of PMMA with 2 mm thickness is used and the actuator is located at $x=470$ mm from the leading edge.

In order to understand the effect of the DBD plasma actuator in the vicinity of the electrodes, the results obtained from a previous study [12] with a similar aerodynamic configuration are worthy of interest. Figure 2 shows the time evolution of the longitudinal velocity component downstream from a DBD actuator when the latter is turned on. In this case, the velocity was measured using Laser Doppler Anemometry (LDA) at $y=1$ mm from the wall and at $x=10$ mm from the downstream edge of the air-exposed electrode. The main flow was seeded with mineral oil particles and the magnitude of the free-stream velocity was very low (3 m/s), resulting in data rates of about 10 kHz.

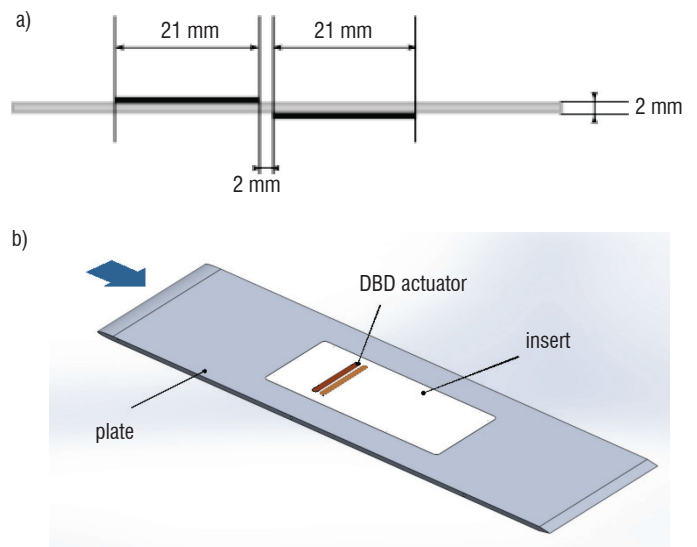


Figure 1 - Cross-section view of a typical DBD actuator used in the DMAE (a) and a flat plate model equipped with one of them (b)

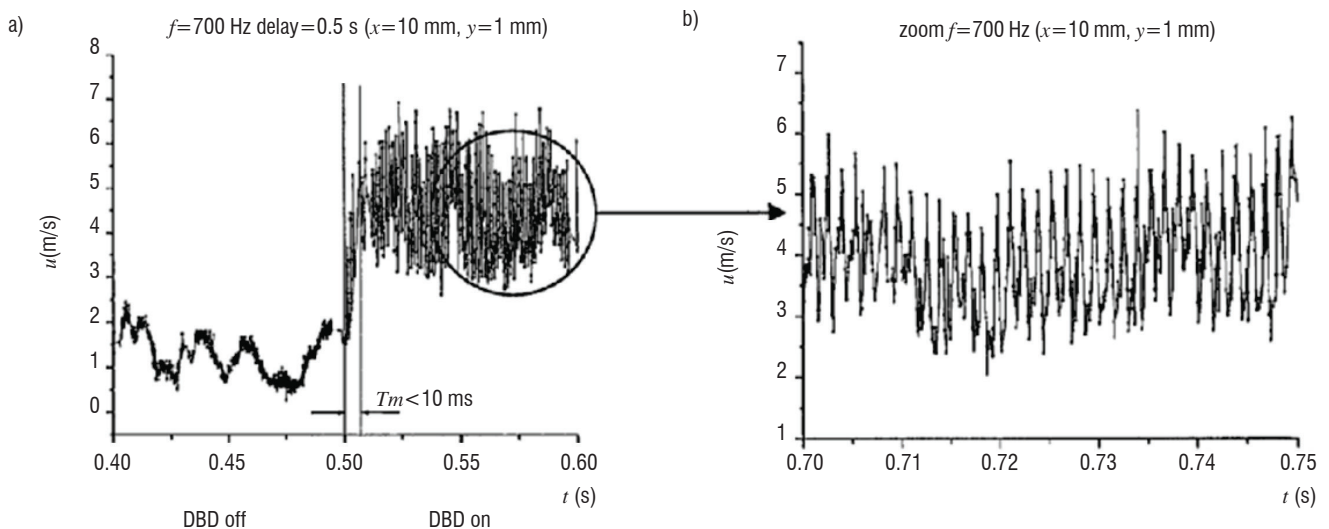


Figure 2 – Time evolution of the longitudinal velocity component downstream from a DBD plasma actuator (a) and with a smaller time scale (b) I, from [12]

Figure 2(a) shows a clear increase in the magnitude of the mean velocity (from 1.5 m/s up to 5 m/s) a few milliseconds after the actuator is turned on. As explained previously, the DBD induces a body force parallel to the wall, which results in a steady wall jet of a few meters per second (often called “ionic wind”). Nevertheless, this steady effect is superimposed with an unsteady effect visible in Figure 2(b), which shows the time evolution of the velocity when the actuator is turned on, and with a smaller time scale. Velocity fluctuations are clearly visible at the same frequency (700 Hz) as the high voltage signal used to supply the actuator. In fact, as has been demonstrated by many authors [1], the DBD actuator induces an unsteady body force at the frequency of the high voltage signal, mainly due to the different discharge regimes between the positive and the negative half cycles.

In the case of a two-dimensional boundary layer, the natural transition is induced by the spatial growth of unsteady instability modes, the well-known Tollmien-Schlichting (TS) waves. If we want to achieve a delay of the transition location, the goal is to decrease this spatial growth or to damp the TS waves. Basically, two approaches are possible to attain this goal: on the one hand, steady actuation is used to modify the mean velocity profile, in order to make the boundary layer more stable. On the other hand, unsteady actuation is used to directly counteract the instabilities. The DBD actuator has the ability of delaying transition by means of either steady or unsteady actuation, as this actuator is able to induce either a quasi-steady or unsteady body force (depending on the electrical parameters of the high-voltage signal) [13]. Most of the results presented in this paper about transition delay are linked with the first approach: stabilization of the boundary layer using the quasi-steady body force induced by the actuator. “Quasi-steady” means that the frequency of the high voltage signal has to be chosen properly at a sufficiently high value, in order to ensure that the unsteady effect will not excite the TS waves, resulting in a promotion of the transition. Thus, only the quasi-steady body force will be considered in the following, assuming that the frequency of the DBD actuator is higher than the most amplified TS frequencies.

Flat plate case

The model shown in Figure 1 is mounted in the TRIN2 wind tunnel of the DMAE, with a free-stream velocity of 35 m/s. This facility features a low turbulence level ($Tu \sim 1.5 \times 10^{-3}$) and is well suited for transition experiments (transitional N-factor ~ 7). Assuming the development of a Blasius boundary layer, the linear stability

theory, which agrees with time-resolved hot-wire measurements, shows that the most unstable TS frequencies range from 600 Hz to 1000 Hz. As a consequence, the frequency of the DBD input signal is set at 3 kHz, a value that is sufficiently above the TS frequencies to assume that only a quasi-steady body force will play a major role. The latter adds momentum inside the boundary layer (in the same direction as that of the main flow) and modifies the mean velocity profile in such a way that it is more stable with respect to the instability TS modes, leading to a transition delay (similarly to when suction is applied) with a global benefit in terms of friction drag.

The study presented in this paper has two main objectives: the first is to establish a model of the body force induced by the DBD actuator and assess the efficiency of the set-up with respect to the laminar-turbulent transition position. The longitudinal velocity component is usually determined by hot-wire measurements inside the boundary layer. However, this kind of measurement is not possible very close to the actuator, because of the interactions between the discharge and the hot-wire probe. Therefore, it has been decided to perform LDA measurements in the vicinity of the actuator. Figure 3 gives an example of such velocity measurements, just above the downstream edge of the air-exposed electrode ($x=470$ mm) without and with actuation for two different values of the electrical power consumption.

Velocity profiles obtained from LDA measurements are represented, compared to the local Blasius boundary-layer profile. These are in very good agreement when the DBD is not active (left graph of Figure 3). When the actuator is turned on, the longitudinal velocity is increased in the boundary layer close to the wall, approximately in the first half of the boundary layer thickness. These measurements clearly show the effect of the steady body force induced by the actuator inside the boundary-layer. The next step is to measure the transition location, in order to assess whether the boundary layer is stabilized by this DBD actuation.

Figure 4 shows the longitudinal evolution of the velocity fluctuations inside the boundary layer at a constant height ($z=1$ mm) above the wall, obtained from hot-wire measurements. This plot presents the same three cases as Figure 3. The transition location is characterized by a sudden increase in the velocity fluctuation, as the boundary-layer regime changes from laminar to turbulent.

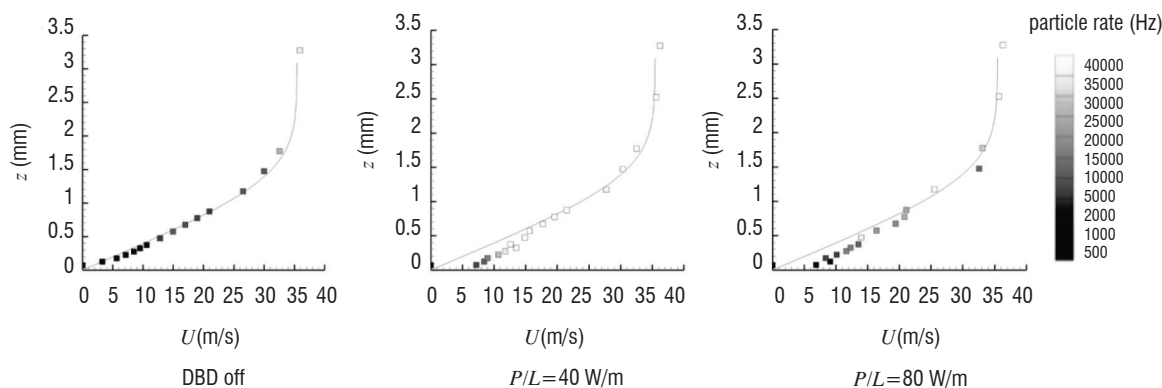


Figure 3 - LDA measurements of the longitudinal velocity just above the DBD actuator in comparison with a Blasius boundary-layer profile (full line) without and with DBD actuation

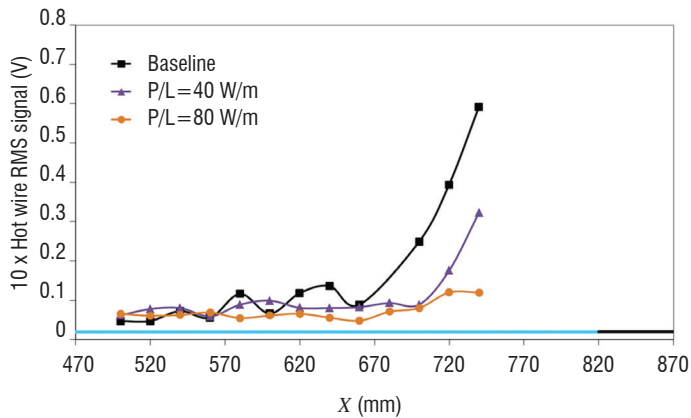


Figure 4 - Longitudinal evolutions of the velocity fluctuations inside the boundary layer without and with DBD actuation

The natural transition location (without actuation) is measured at $x=670$ mm. When the actuator is turned on, the transition location is progressively shifted downstream when the power consumption of the actuator is increased. For the lowest power consumption, the transition location is delayed by roughly 35 mm, and by more than 80 mm in case of the highest power value. These measurements prove that the local modification of the velocity profiles induced by the actuator (shown in Figure 3) enables the stabilization of the boundary layer and a delay in the transition.

2D airfoil case

The same kind of DBD actuator has also been installed on an airfoil model based on an ONERA-D profile, as presented in Figure 5 (left). The goal of this study was to assess the ability of the actuator to control the transition on a more realistic aerodynamic configuration, for which the boundary layer develops with a non-zero pressure gradient. The model is mounted inside the TRIN1 wind tunnel of the DMAE with an incidence of 1.5° in an unswept configuration. Longitudinal hot-wire measurements have been performed inside the boundary layer at a constant height above the wall, similarly to the measurements presented in Figure 4, and for a free-stream velocity of 21 m/s. The longitudinal evolutions of velocity fluctuations are shown in Figure 5 (right), without and with actuation, for a DBD actuator located at $x/c=33\%$.

The results presented in Figure 5 (right) are very similar to those shown in Figure 4: the transition is progressively shifted downstream when the actuator is turned on and when the electrical power is increased. A maximum transition delay of 6% of the chord has been measured for the highest power consumption value.

This experiment has been reproduced numerically, using the experimental pressure distribution to perform boundary-layer computations and linear stability analysis. A model of the body force induced by the DBD actuator has been implemented in a boundary-layer code, so as to study the influence of the plasma actuator on the stability of the boundary layer. An example of a numerical result is shown in Figure 6, which presents the chordwise evolutions of the N-factors (chordwise integration of amplification rate) for various instability frequencies without (left) and with (right) actuation, using similar conditions as for the experiment.

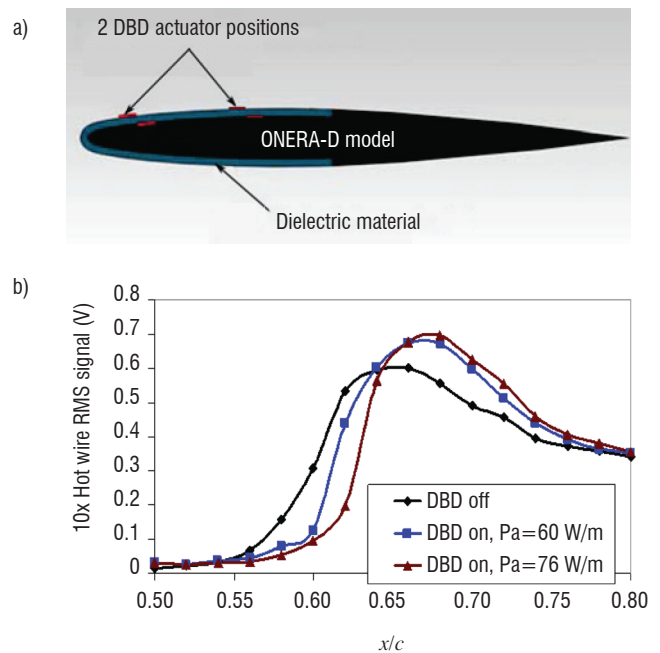


Figure 5 - (a) Cross-sectional view of the ONERA-D model equipped with DBD actuators (b) longitudinal evolutions of velocity fluctuations inside the boundary layer without and with DBD actuation

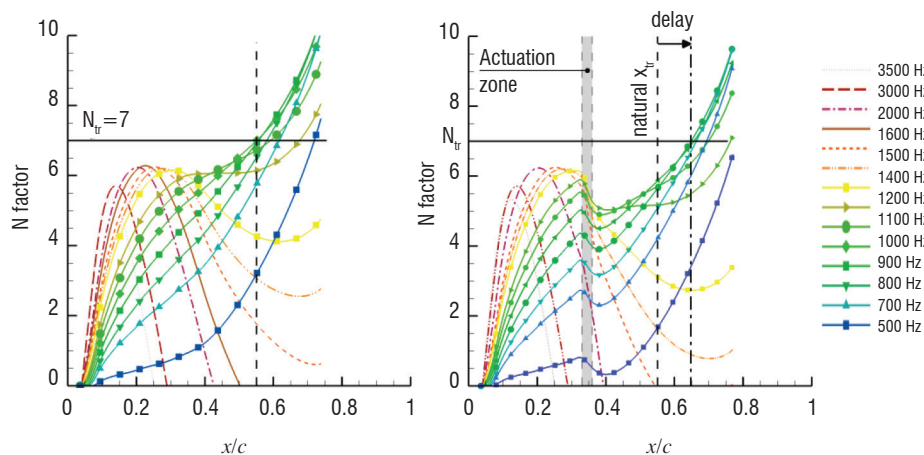


Figure 6 - Linear stability analysis of the boundary layer developed on the ONERA-D model for the baseline case (left) and with DBD actuation (right - $P_a=60$ W/m) for a free-stream velocity of 21 m/s

Using the natural transition location obtained from the experiment ($x_{tr}/c=56\%$ in Figure 5), the left part of Figure 6 enables the value of the transitional N-factor ($N_t=7$) to be determined, which corresponds to the transition threshold in the well-known eN method [14]. Then, using the body force model, the manipulated boundary layer was computed and the corresponding stability analysis has been plotted in Figure 6 (right). The stabilizing effect on the TS waves is clearly visible, since all of the N-factor curves are decreasing in the region of the plasma-induced body force, resulting in a transition delay of 8% of the chord. The numerical results slightly overestimate the experimental delay.

Current work and perspectives

With the perspective of delaying the laminar-turbulent transition along the wings of realistic transportation airplanes, another issue is to deal with crossflow instabilities. Indeed, given that real wings have a non-zero sweep angle, the boundary layer is 3D and the mean velocity profile in the direction perpendicular to the external streamlines – the so-called crossflow direction – exhibits an inflection point inside the boundary layer. This induces a strong disturbance called the crossflow (CF) instability, which occurs close to the leading edge for accelerated mean flows. For this particular instability, both unsteady and steady modes can be spatially amplified in the streamwise direction. The steady crossflow instability amplitudes are strongly related to the roughness of the surface on which the considered boundary layer is developing. Finally, two approaches are currently being investigated in order to control the crossflow induced transition: the first is to modify the mean crossflow velocity profile inside the boundary layer; the second is to use nonlinear interactions between several crossflow instabilities.

The first approach has been investigated for many years using wall suction. The mean velocity profile modified by suction is more stable with respect to the instability modes, inducing a delay of the transition location. This idea has been tested in-flight by several industrial aircraft manufacturers and has proven to be very efficient for transition delay. However, all of the devices used to create the suction are quite expensive to implement in practice, so alternative ways must also be assessed. The DBD actuator seems to be a promising way: given that the intensity of the mean CF velocity profile is not very high, it can reasonably be affected by the body force induced by this kind of plasma actuator. Of course, the direction of the induced body force must be chosen properly, so as to reduce the magnitude of the inflexional CF mean velocity profile.

The second possible approach is to use the DBD actuator to mimic micron-roughness elements, in order to induce a non-linear interaction between the artificial CF modes and the natural modes leading to transition. Previous experiments performed in the US [15] and in the DMAE [16] show that using artificial roughness elements regularly stuck in a line parallel and close to the leading edge, forces the steady CF instability vortices, with the spanwise wavelength corresponding the spacing between two consecutive roughness elements. Then, the trick consists in exciting a slightly amplified CF mode in such a way that a non-linear interaction modifies the mean velocity profile, which becomes more stable with respect to the most amplified CF modes. This idea has been successfully implemented experimentally but the size of the roughness elements must be chosen very accurately. The

advantage of using DBD actuators instead of these roughness elements is that the amplitude of the body force can be adjusted.

Both ways are currently being investigated within the framework of the BUTERFLI European Project, in cooperation with Russia.

Plasma Synthetic Jet actuator

For several years, the DMAE [17,18], in collaboration with the CNRS LAPLACE laboratory [19,20], has developed the Plasma Synthetic Jet (PSJ) actuator, shown in Figure 7, which is similar to the SparkJet actuator [21]. This is a compact actuator designed to be integrated into a wall and dedicated to flow control applications. It consists of a cylindrical cavity whose dimensions do not exceed a few millimeters. A convergent nozzle is added to produce a jet, as explained in the following, which interacts with the external flow. The exhaust orifice has a diameter of 1 mm. Two electrodes are located inside the cavity and are connected to an electric circuit. Figure 8 shows a diagram of the actuator and the electric circuit. The latter can be decomposed into two parts: the charge circuit consisting of a high voltage pulse generator, a resistance R_c and a capacitor C , and the discharge circuit consisting of the same capacitor and the electrodes. At the beginning of a cycle, the capacitor is discharged and a high voltage pulse is produced by the power supply. The voltage at the capacitor increases up to the breakdown voltage value of the air surrounding the electrodes. At this instant, an electric arc is produced between the electrodes. Due to the Joule effect, the resulting plasma arc transfers energy to the air inside the cavity. The temperature and the pressure increase inside the cavity. A jet is then generated through the nozzle. Afterwards, a natural suction phase occurs, driven by simple pressure recovery, and the cycle can be repeated. Thus, the PSJ actuator works as a zero net mass flux device. When the actuation frequency is high enough, the operation of the PSJ during a cycle is influenced by the previous cycle. In this case, at the breakdown instant, the air inside the cavity is not at rest. Also, the temperature of the air inside the cavity, the walls and the electrodes may remain high. The energy deposition is modified by these high-frequency effects, as well as the dynamics within the cavity. As a consequence, when the frequency is high enough, the jet generated is different from that generated by the PSJ working in a single-pulse or low-frequency mode.



Figure 7 – Photograph of a PSJ actuator

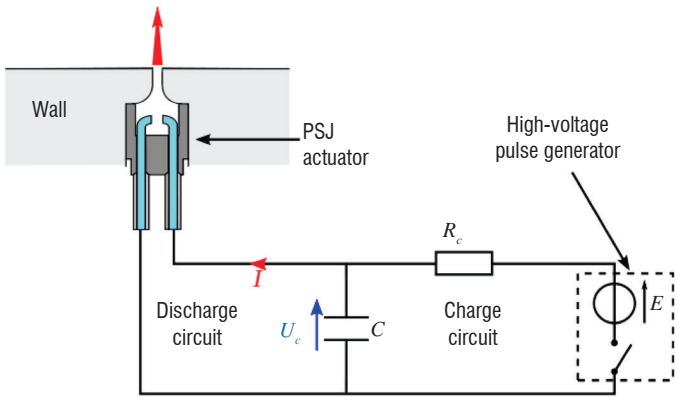


Figure 8 – Diagram of the PSJ actuator inserted into a wall, defining the boundary of a flow, and its electric power supply

Experimental characterization

A significant number of experimental characterizations have been conducted at the DMAE on the jet produced by a PSJ actuator, either with or without a flow on the surface of the wall in which it is inserted. While the experiments bringing into play a flow have shown the capability of the actuator to alter and control its dynamics, this section is focused on the characterizations performed in a quiescent environment. Indeed, in order to build an accurate model of the PSJ actuator, a first necessary step is to capture the dynamics of the synthetic jet without any external influences.

Electrical measurements

In order to characterize the electric discharge that drives the energy deposition inside the cavity of the PSJ actuator, and thus ultimately the dynamics of the synthetic jet, measurements of the capacitor voltage U_c and the current in the discharge circuit I were performed with a PSJ actuator working at a repetition rate of 1Hz. This frequency is sufficiently low to consider the actuator as working in a single-pulse mode. An example of the signals obtained for a capacitance $C = 12.2$ nF is provided in Figure 9. The voltage across the capacitor initially follows the expected charging of the RC series circuit previously described in Figure 8. The discharge circuit being open, the current is null. At about $t = 11.5 \mu\text{s}$, electrical breakdown occurs and the plasma generated between the electrodes closes the discharge circuit: the voltage across the capacitor U_c and the discharge intensity I then describe underdamped oscillatory responses, indicative of a spark discharge [19,22]. Based on a large number of measurements, we showed that a simple and relevant electrical model of the discharge can be constructed to reproduce the major characteristics of the current during the energy deposition phase of the PSJ actuator. This electrical model of the discharge is shown in Figure 10. Particularly, it can be assumed that the total equivalent resistance R and inductance L are constant during the discharge. This model will serve as a physically-based input for unsteady simulations of the actuator relying on the methodology proposed by Laurendeau et al [23], and sheds light on the major electrical parameters driving the discharge, which it is important to account for in future design improvements of the actuator.

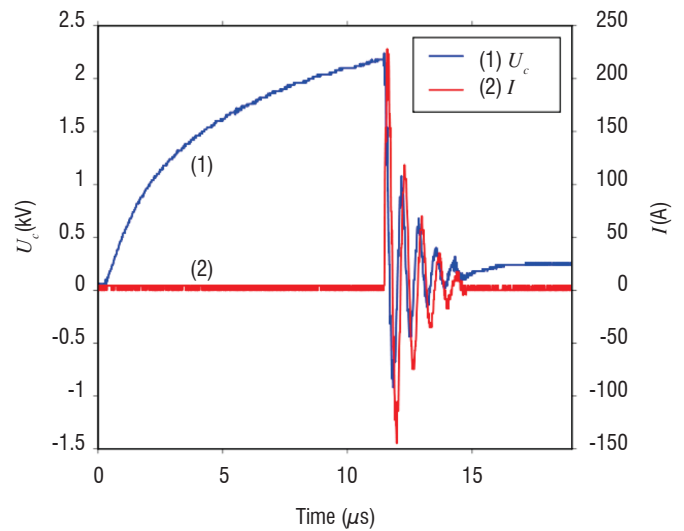


Figure 9 - Capacitor voltage U_c and current in the discharge circuit I measured during one actuation cycle with an effective capacitance $C = 12.2$ nF

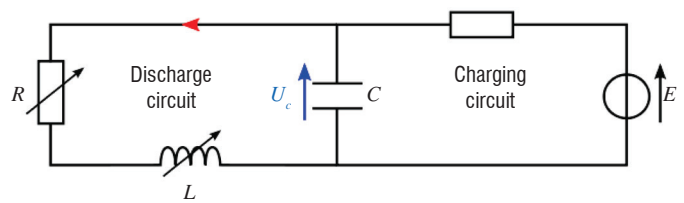


Figure 10 - Equivalent electrical model of the PSJ actuator power supply during the arc discharge, where R and L respectively refer to the total resistance and inductance in the discharge circuit induced by the wires and plasma

Schlieren visualizations

A first aerodynamic characterization of the synthetic jet produced in a quiescent environment was performed using Schlieren visualizations. Such visualizations are aimed at providing a qualitative description of the density gradients in a given direction, integrated along the path of the rays of light. Examples of Schlieren visualizations obtained for a capacitance of 30 nF are provided in Figure 11. A phase-averaging procedure was used, in order to provide the mean jet topology at given instants during its development. The phase-averaging process is performed using the breakdown instant as the reference instant. As observed in these figures, the phase-averaged synthetic jet is composed of a train of vortex rings, convected at different velocities and interacting with one another. The generation of these vortex rings is tightly linked to the dynamics of the pressure waves generated inside the cavity of the actuator during the energy deposition phase.

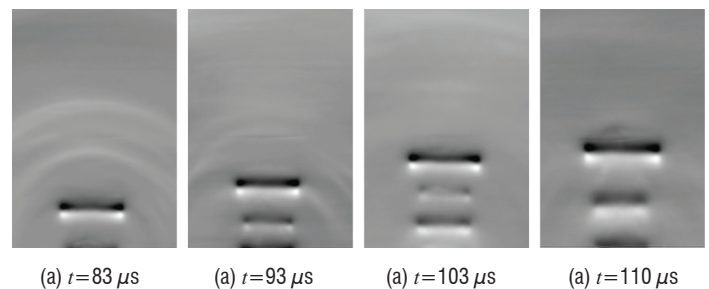


Figure 11 - Phase-averaged Schlieren visualizations obtained for an installed capacitance $C = 30$ nF, at various instants t from the breakdown instant.

Particle Image Velocimetry

A more quantitative characterization was then conducted for the synthetic jet produced by the actuator, through Particle Image Velocimetry (PIV). A diagram of the setup used is shown in Figure 12. Performing a high-quality PIV measurement of such a synthetic jet requires some challenges to be overcome, particularly regarding the seeding of the jet [24] and the evaluation of the sources of uncertainty. Indeed, first with regard to the seeding, the air inside the cavity of the actuator cannot be seeded directly for geometrical reasons and the particles tend to be naturally expelled from the synthetic jet. Although the vortex rings drag particles in the jet core, this results in poorly seeded areas in instantaneous PIV images. However, through a phase-averaged approach it can be expected to provide sufficient information to yield a satisfactory averaged description of the complete jet velocity field. This approach was thus selected for these measurements. Second, regarding the sources of uncertainty in such measurements, various parameters must be accounted for. The major parameters identified were the location of the laser sheet (about 0.4 mm thick) with respect to the actuator exit orifice (diameter of 1 mm), the position of the wall on the images and the dispersion of the velocity calculated by the PIV algorithm. The uncertainty analysis conducted [25] then allows these measurements to be compared with simulations of the actuator.

An example of the PIV measurements obtained with an effective capacitance value $C = 10.2$ nF is shown in Figure 13. In this figure, the evolution of the axial velocity, the radial velocity and the vorticity are presented for 3 consecutive instants measured as from the breakdown instant. With this capacitance, phase-averaged axial velocities up to 120 m/s are reached

on the jet axis. The generation of a train of vortex rings can be observed on the vorticity maps, with the circled numbers localizing the different rings. As observed with the Schlieren visualizations, the vortex rings interact, but at different instants due to the difference in capacitance values.

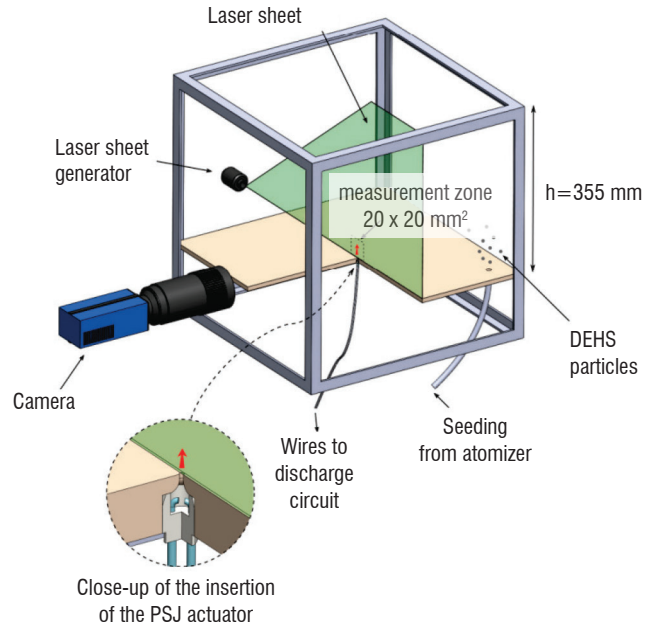


Figure 12 – Diagram illustrating the PIV setup and the flow visualization chamber; a quarter of the floor in which the PSJ actuator is inserted was removed for clarity

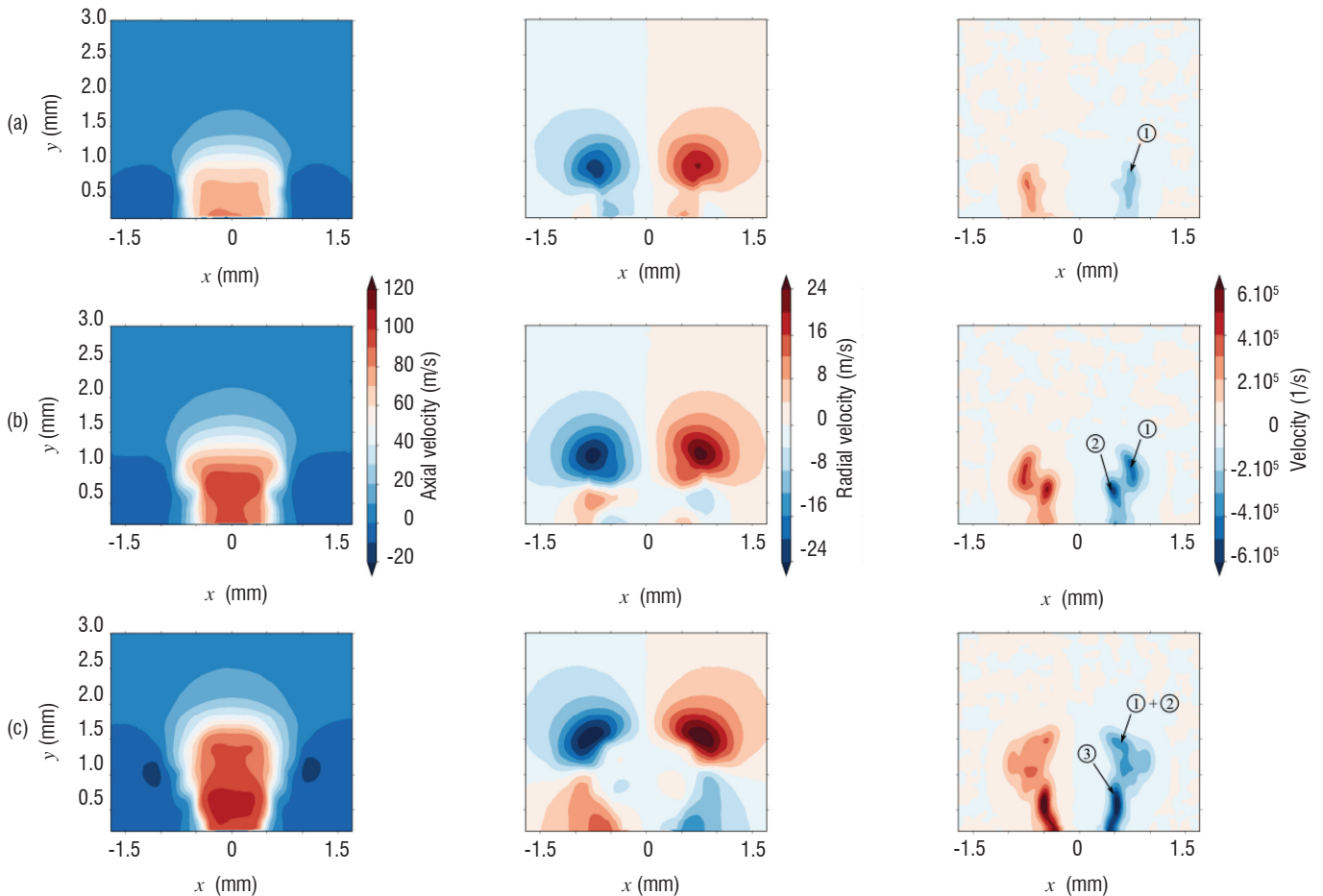


Figure 13 – Contour maps of the phase-averaged axial velocity (left column), radial velocity (center column) and vorticity (right column), obtained for an effective capacitance $C=10.2$ nF, at various instants in the jet development: (a) $t = 56.3 \mu\text{s}$, (b) $t = 66.1 \mu\text{s}$, (c) $t = 76.1 \mu\text{s}$. On the vorticity maps, the circled numbers highlight specific vorticity regions identified as vortex rings.

LES methodology

Contrary to DBD models, for which non-equilibrium plasma physics is required, the PSJ actuator induces plasma, for which the LTE (Local Thermodynamic Equilibrium) hypothesis can be formulated. Such an assumption eases the development of a dedicated model since the flow and the plasma can be considered as a unique mixture driven by a real gas law. Thus, following the work initiated by Sary et al [26], the spark discharge is modeled through energy source terms depending on time and space, and introduced into a large eddy simulation. The current intensity being known, whether from direct measurement or through an equivalent RLC circuit [14], the source term S is written as:

$$S = \sigma E^2$$

where σ is the electric conductivity and E is the electric field:

$$E = \frac{I}{\int_0^{r_{arc}} 2\pi r \sigma dr}$$

The discharge canal is assumed to be cylindrical, with a radius r_{arc} . Due to the high temperature generated by the energy deposition, a real gas model is adopted for air in the computation. The model selected is that proposed by D'Angola et al [27], for which, for example, the electric conductivity is a function of the pressure and the temperature. Thus, the source term S is coupled to the Navier-Stokes solver for the gas, which provides the spatial distribution and the temporal evolution of the pressure and the temperature. From these data, the source term is evaluated in the fluid domain and added to the energy equation.

The CEDRE code [28] from ONERA is a multi-physics platform that contains several solvers, all coupled together. The source term S is computed from a solver called COPAIER, included in the CEDRE code, and coupled to the unstructured Navier-Stokes solver called CHARME. In order to compute the synthetic jet produced by the energy deposition inside the cavity, Large Eddy Simulations (LES) are carried out. The cavity, including the electrodes, is meshed with about one million cells, as shown in Figure 14, whereas the outer region in which the jet expands typically contains 5-10 million cells.

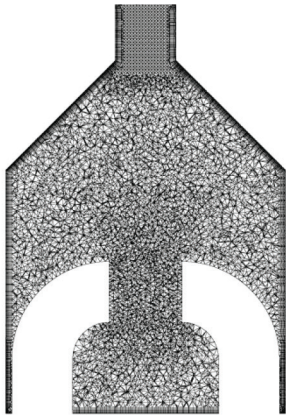


Figure 14 - Typical mesh inside the PSJ cavity

Excellent agreement with measurements from Hardy et al [8] has been obtained by Laurendeau et al [23]. Comparisons of the jet front evolution and jet topology have proven the relevance of the proposed methodology. Recently, further validation of the energy deposition model has been achieved using the PIV measurements. Figure 15 compares velocity fields obtained from PIV and from the LES at the same instant after the breakdown.

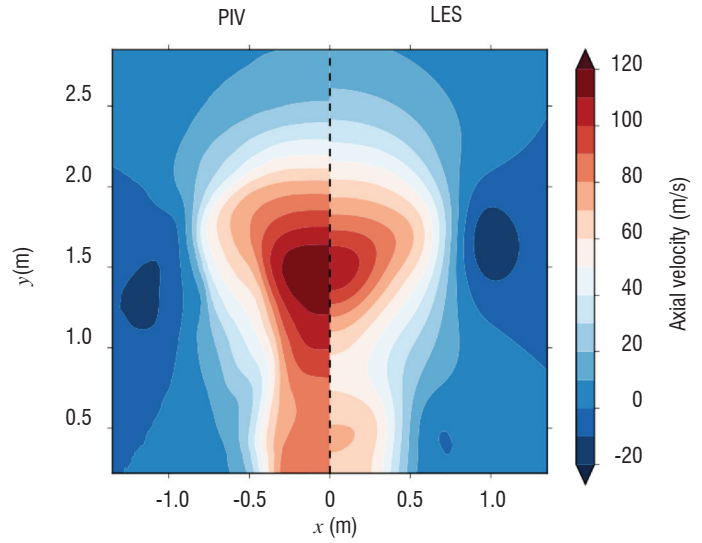


Figure 15 - Axial velocity fields V_y generated with a capacitance value $C = 10.2$ nF. Left: phase-averaged velocity measured by PIV at $t = 86.1 \mu\text{s}$. Right: velocity yielded by LES at $t = 86.1 \mu\text{s}$ after the breakdown.

The general topology of the synthetic jet is well recovered and the velocity magnitudes are also fairly well reproduced. Main discrepancies appear in zones where the confidence level is rather low for PIV measurements [25].

Conclusion

For several years, ONERA has investigated both DBD and PSJ plasma actuators. Two different objectives have been targeted: the transition location delay for a DBD actuator and the separation reduction or delay for a PSJ actuator. The ONERA approach consists in a dual investigation relying on both dedicated experimental work and CFD simulations. For the DBD actuator only a heuristic model is under development at the DMAE, with the goal of implementing it in CFD codes. On the other hand, a detailed model of the PSJ actuator is being investigated, using LES simulations. A very good agreement has been obtained when comparing the results of the simulations with PIV measurements, inducing a reasonable trust in the energy deposition model. The next step will consist in deriving a simple model of the flow at the exhaust of the PSJ actuator, this model being then implemented in CFD codes for practical applications of flow active control. Using both experiments and numerical simulations, Onera intends to implement control strategies based on these plasma devices in complex and realistic aerodynamic configurations ■

Acknowledgements

First investigations regarding the plasma actuators in DMAE have been performed in the European project PLASMAERO. Most of the presented results come from the PhD works of Natacha Szulga and Francois Laurendeau, both granted by DGA and ONERA.

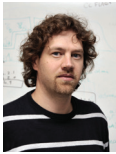
References

- [1] N. BENARD, E. MOREAU - *Electrical and Mechanical Characteristics of Surface AC Dielectric Barrier Discharge Plasma Actuators Applied to Airflow Control*. Experiments in Fluids 55:1846 (2014)
- [2] M. FORTE, A. DEBIEN, D. CARUANA, N. BENARD, PH. BARRICAU, CH. GLEYZES, E. MOREAU - *Mid-Chord Separation Control Using PSJ and DBD Plasma Actuators*. ERCOFTAC Bulletin, vol. 94, pp. 41-46, March (2013).
- [3] S. GRUNDMANN, C. TROPEA - *Experimental Transition Delay Using Glow-Discharge Plasma Actuators*. Experiments in Fluids 42(4):653-657 (2007).
- [4] R. JOUSSOT, R. WEBER, A. LEROY, D. HONG - *Transition Control Using a Single Plasma Actuator*. International Journal of Aerodynamics, 3 (2013).
- [5] A. DUCHMANN, S. GRUNDMANN, C. TROPEA - *Delay of Natural Transition with Dielectric Barrier Discharges*. Experiments in Fluids 54(3):1-12 (2013).
- [6] A. SÉRAUDIE, O. VERMEERSCH O., D. ARNAL - *DBD Plasma Actuator Effect on a 2D Model Laminar Boundary Layer*. Transition delay under ionic wind effect. AIAA Applied Aerodynamics Conference (2011).
- [7] A. DUCHMANN, B. SIMON, C. TROPEA, S. GRUNDMANN - *Dielectric Barrier Discharge Plasma Actuators for In-Flight Transition Delay*. AIAA Journal 52(2):358-367 (2014).
- [8] W. SHYY, B. JAYARAMAN, A. ANDERSSON - *Modeling of Glow Discharge-Induced Fluid Dynamics*. Journal of applied physics 92(11):6434-6443 (2002).
- [9] K.P. SINGH, S. ROY - *Force Approximation for a Plasma Actuator Operating in Atmospheric Air*. Journal of Applied Physics 103(1):0133051-0133056 (2008).
- [10] T. UNFER, J.P. BOEUF - *Modeling and Comparison of Sinusoidal and Nanosecond Pulsed Surface Dielectric Barrier Discharges for Flow Control*. Plasma Physics and Controlled Fusion 52:124019 (2010).
- [11] J. KRIEGSEIS, C. SCHWARZ, C. TROPEA, S. GRUNDMANN - *Velocity-Information-Based Force-Term Estimation of Dielectric-Barrier Discharge Plasma Actuators*. Journal of Physics D: Applied Physics 46(5):055202. (2013).
- [12] M. FORTE, L. LEGER, J. PONS, E. MOREAU, G. TOUCHARD - *Plasma Actuators for Airflow Control: Measurement of the Non-Stationary Induced Flow Velocity*. Journal of Electrostatics, 63(6), 929-936 (2005).
- [13] A. KURZ, S. GRUNDMANN, C. TROPEA, M. FORTE, A. SÉRAUDIE, O. VERMEERSCH, D. ARNAL, N. GOLDIN, R. KING - *Boundary Layer Transition Control Using DBD Plasma Actuators*. AerospaceLab Journal Issue 6, AL06-02 (2013).
- [14] A. SMITH, N. GAMBERONI - *Transition, Pressure Gradient and Stability Theory*. Douglas Aircraft Co. Rept. ES 26388, El Segundo, California (1956).
- [15] W.S. SARIC, A.L. CARPENTER, H. REED - *Passive Control of Transition in Three-Dimensional Boundary Layers, with Emphasis on Discrete Roughness Elements*. Phil. Trans. R. Soc. A 369:1352-1364 (2011).
- [16] O. VERMEERSCH, D. ARNAL, E.I. ALAH, L. DIN - *Transition Control by Micron-Sized Roughness Elements: Non-Linear Stability Analyses and Wind Tunnel Experiments*. International Journal of Engineering Systems Modelling and Simulation 5(1-3/2013):84 (2013).
- [17] P. HARDY, PH. BARRICAU, A. BELINGER, D. CARUANA, J.P. CAMBRONNE, CH. GLEYZES - *Plasma Synthetic Jet for Flow Control*. 40th Fluid Dynamics Conference and Exhibit, AIAA 2010-5103 (2010).
- [18] D. CARUANA, F. ROGIER, G. DUFOUR, CH. GLEYZES - *The Plasma Synthetic Jet Actuator, Physics, Modeling and Flow Control Application on Separation*. AerospaceLab Journal Issue 6, AL06-10 (2013).
- [19] A. BELINGER, P. HARDY, PH. BARRICAU, J.P. CAMBRONNE, D. CARUANA - *Influence of the Energy Dissipation Rate in the Discharge of a Plasma Synthetic Jet Actuator*. J Phys D Appl Phys 44:365-201 (2011).
- [20] A. BELINGER, P. HARDY, N. GHERARDI, N. NAUDE, J.P. CAMBRONNE, D. CARUANA - *Influence of the Spark Discharge Size on a Plasma Synthetic Jet Actuator*. IEEE T Plasma Sci 39:2334-2335 (2011).
- [21] K. GROSSMAN, B. CYBYK, D. VANWIE - *Sparkjet Actuator for Flow Control*. 41st Aerospace Sciences Meeting and Exhibit, AIAA 2003-57 (2003).
- [22] W.D. GREASON - *Methodology to Study the Resistance of a Spark Discharges*. IEEE T Ind Appl 35(2):359-365 (1999).
- [23] F. LAURENDEAU, F. CHEDEVERGNE, G. CASALIS - *Transient Ejection Phase Modeling of a Plasma Synthetic Jet*. Physics of Fluids 26(12):125,101 (2014).
- [24] T.M. REEDY, N.V. KALE, J.C. DUTTON, G.S. ELLIOT - *Experimental Characterization of a Pulsed Plasma Jet*. AIAA Journal 51(8):2027-2031 (2013).
- [25] F. LAURENDEAU, O. LÉON, F. CHEDEVERGNE, G. CASALIS - *PIV and Electric Characterization of a Plasma Synthetic Jet Actuator*. 45th AIAA Fluid Dynamics Conference, AIAA 2015-2465 (2015).
- [26] G. SARY, G. DUFOUR, F. ROGIER, K. KOURTZANIDIS - *Modeling and Parametric Study of a Plasma Synthetic Jet for Flow Control*. AIAA Journal Vol 52 ,no 8, pp 1591-1603 (2014).
- [27] A. D'ANGOLA, G. COLONNA, C. GORSE, M. CAPITELLI - *Thermodynamic and Transport Properties in Equilibrium Air Plasma in a Wide Pressure and Temperature Range*. Eur. Phys. J. D, vol 46, pp 129-150 (2007).
- [28] A. REFLOCH, B. COURBET, A. MURRONE, PH. VILLEDIEU, C. LAURENT, P. GILBANK, J. TROYES, L. TESSÉ, G. CHAINERAY, J.B. DARGAUD, E. QUÉMERIS, F. VUILLOT - *CEDRE Software*. AerospaceLab Journal Issue 2, AL02-11 (2011).

Acronyms

| | |
|------|-----------------------------------|
| DBD | (Dielectric Barrier Discharges) |
| PSJ | (Plasma Synthetic Jet) |
| RANS | (Reynolds Averaged Navier-Stokes) |
| LDA | (Laser Doppler Anemometry) |
| TS | (Tollmien-Schlichting) |
| CF | (Crossflow) |
| PIV | (Particle Image Velocimetry) |
| LES | (Large Eddy Simulations) |
| CFD | (Computational Fluid Dynamics) |

AUTHORS



François Chedevergne graduated from ISAE SUPAERO, France, and received his PhD degree in Fluid Mechanics in 2007. He is in charge of the modeling of the PSJ actuator developed at ONERA. He is also involved in the development of the ONERA code CEDRE, concerning all aspects related to turbulence modelling.



Grégoire Casalis is the Scientific Deputy Director of the Department Modelling in Aerodynamics and Energetics of ONERA. He is Professor at ISAE-Supaero and has been the director of the Doctoral School "Aeronautics-Astronautics". His scientific topics are related to flow stability, from generic configurations (laminar boundary layer) to complex ones (internal solid rocket motor flow).



Olivier LÉON graduated from École Centrale de Lyon, France, and simultaneously obtained his M.Sc. degree in Aerospace Engineering from the Pennsylvania State University, USA, in 2009. He obtained his Ph.D. degree in Fluid Mechanics in 2012 from Toulouse University. His research interests include fluid dynamics metrology and flow control using plasma actuators.



Maxime Forte graduated from Ecole Nationale Supérieure de Mécanique et d'Aérotechnique (ENSMA - French engineering school specialized in space and aeronautics) in 2004 and received his PhD in Fluid Mechanics from the University of Poitiers in 2007. He joined ONERA in 2010 and works as a research scientist in the Aerodynamics and Energetics Modeling Department in Toulouse. His research interests include experimental investigations on boundary-layer transition (flow control, tripping criteria and new devices for transition detection).



François Laurendeau obtained his engineering degree from SUPAERO in 2013. He is currently a PhD student at Onera. His work, co-financed by the Direction Générale de l'Armement, deals with the unsteady simulations and the PIV characterizations of the Plasma Synthetic Jet actuator.



Natacha Szulga graduated from ISAE-ENSICA in 2013 and is now a PhD student at ONERA-DMAE. Her current work deals with boundary layer transition control by means of DBD actuation and is funded by ONERA and DGA (Délégation Générale de l'Armement).



Olivier Vermeersch graduated from École Nationale Supérieure de Mécanique et d'Aérotechnique (ENSMA - French engineering school specialized in space and aeronautics) in 2006 and received his PhD in Fluid Mechanics from the University of Toulouse in 2009. Since then, he has worked as a research scientist in the Aerodynamics and Energetics Modeling Department of Onera. His research interests include boundary-layer stability computations and control of the laminar/turbulent transition with different kinds of actuation (micro-sized roughnesses, plasma actuators).



Estelle Piot graduated in 2005 from Ecole Polytechnique in Paris, and received her PhD in Fluid Mechanics from the University of Toulouse/Supaéro in 2008, for studies of boundary layer instabilities. Since then, she has been a research engineer at ONERA, in charge of aeroacoustics characterization and optical measurements in flow ducts. In 2014, she became the head of Instability, Transition and Acoustics research unit.